Upcycling of lignin waste to activated carbon for supercapacitor electrode and organic adsorbent

Youn-Ki Lee*,**,‡, Sangchul Chung****,‡, Sang Youp Hwang*****, Sungho Lee*, Kwang Sup Eom**,
Seung Bin Hong***, Gwan Gyu Park***, Byung-Joo Kim******, Jung-Joon Lee****,†, and Han-Ik Joh***,†

*Carbon Composite Materials Research Center, Korea Institute of Science and Technology (KIST),
92 Chudong-ro, Bongdong-eup, Wanju-gun, Jeollabuk-do 55324, Korea
**School of Materials Science and Engineering, Gwangju Institute of Science and Technology (GIST),
123 Cheomdangwagi-ro, Buk-gu, Gwangju 61005, Korea
***Department of Energy Engineering, Konkuk University, 120 Neungdong-ro, Gwangjin-gu, Seoul 05029, Korea
****Research and Development Center, GS Caltex Corporation, 359, Expo-ro, Yuseong-gu, Daejeon 34122, Korea
*****Plant Engineering Division, Institute for Advanced Engineering, 175-28 Goan-ro 51,
Baegam-myeon, Cheoin-gu, Yongin-si, Gyeonggi-do 17180, Korea
******Research Center for Carbon Convergence Materials, Korea Institute of Carbon Convergence Technology,
Jeonju 54853, Korea
(Received 26 April 2019 • accepted 9 July 2019)

Abstract−We introduce a facile strategy to upcycle lignin waste to valuable activated carbon (AC). Unlike conventional preparation processes of AC, such as high-temperature carbonization above 600 °C followed by chemical or physical activation, we synthesized AC through low-carbonization (~300 °C), ball-milling, and thermal activation. Low-temperature carbonization effectively led to the formation of the micro-pores and simultaneously high yield. Uniform activated morphology of char lignin is achieved through a ball-milling process. The as-synthesized AC exhibited a large specific surface area of 1075.18 m^2 g^{-1}, high specific capacitance of 115.1 F g^{-1}, and excellent adsorbability of 0.23 $g_{toluene}$ per $g_{activated\ carbon}$. Therefore, we believe that the presented facile strategy could lead to the realization of upcycling of lignin waste to highly useful AC.

Keywords: Lignin, Activated Carbon, Steam Activation, Capacitor, Volatile Organic Compounds

INTRODUCTION

Lignin is a type of complex organic polymer, which is an abundant source of aromatic chemicals, with carbon content above 60% [1,2]. Generally, lignin is a major component of plant cell walls, which protects the plants from chemical or biological attacks. Thus, the produced amount of lignin varies with the type of plant. It is expected that more than 70 million tons of commercial lignin is produced annually as a by-product of the paper and pulping industries and biorefineries [3,4]. Lignin waste, a type of residue from the extraction processes of cellulose and hemicellulose from non-edible biomass, is composed of various aromatic chemicals. In the case of a biobutanol plant, the maximum lignin production was 35 wt% with respect to the feeding biosources. Despite the high levels of lignin production, its uncharacterized complex structure, such as heterogeneous molecular weight and various functional groups, leads to the application of lignin waste as feedstock for thermal power generation or to its being discarded in landfills.

Considering price competitiveness and environmental effects of lignin, it could be an attractive precursor to prepare highly useful

carbon materials, such as activated carbon (AC), carbon fibers, and graphitic carbon. Among the materials, AC derived from lignin has been widely used in various fields, such as catalyst supports, supercapacitor electrodes, gas separators, adsorbent, filters, and even additives in automobile tires [5-12]. ACs are porous materials with large surface area controlled by physical or chemical activation processes. In physical activation, conventionally using carbon dioxide or steam, AC derived from lignin is prepared by high-temperature carbonization at above 600 °C followed by activation at temperatures ranging from 900 to 1,200 °C [13]. In chemical activation using chemical reagents, such as $ZnCl_2$, H_3PO_4, and KOH, a mixture of lignin and the reagents is heat-treated at a high temperature (>500 °C), leading to the formation of porous carbon materials with large surface area and many pores of various size [14-16]. Both activations could affect the variation in the porosity. Considering the production cost of commercialized processes, physical activation has more advantages over chemical activation, in which washing should be conducted to remove the impurities originating from chemical reagents with corrosive properties [17]. However, long-term activation is required to produce AC with high porosity, owing to the low reactivity of the lignin chars that were prepared in the first step of physical activation. Rodriguez-Mirasol et al. prepared AC from eucalyptus kraft lignin by activation at 850 °C for 20 h [18]. Owing to the long-term activation, the carbon showed a specific surface area of 1,853 m^2 g^{-1}

and a micropore volume of 0.53 m^3 g^{-1}. Some studies also reported that the surface area could be increased by low heating rates [19, 20]. Therefore, the time-consuming activation process could be improved by using lignin as a cost-effective and environmentally friendly precursor in terms of the mass-production of AC. Furthermore, as-synthesized AC would be useful in applications as the capacitor and organic adsorbent.

In this study, we introduce a facile strategy to upcycle lignin waste to valuable AC, suitable for supercapacitor electrodes and organic adsorbent, via low-temperature carbonization, a ball-milling process to increase exposed surface area, followed by an activation process. Carbonization at 300 °C and ball-milling for 12 h significantly affect the formation of lignin char, with relatively large surface area and large reaction sites to activate with steam, respectively, leading to a specific surface area of 1,075.18 m^2 g^{-1} and a total pore volume of 0.732 cm^3 g^{-1}. The AC also exhibited a high specific capacitance of 115.1 F g^{-1}, and an excellent adsorbability of 0.23 $g_{toluene}$ per $g_{activated\ carbon}$. Therefore, we believe that the facile strategy could lead to the realization of upcycling of lignin waste to highly useful AC.

EXPERIMENTAL

1. Synthesis of Activated Carbon

Lignin used in this study was provided by GS Caltex. Lignin was obtained as a side-product, resulting from the pretreatment, and hydrolysis process, which produces sugar using concentrated sulfuric acid hydrolysis of biomass feedstock (Pinus). Lignin powder was carbonized in a furnace under an inert atmosphere (N_2). The temperature was ramped to 300 and 600 °C at 5 °C min^{-1}, and then held constant for 1 h. The yields of carbonized lignin were 40.96, and 30.27 wt% after carbonization at 300, and 600 °C. Subsequently, carbonized lignin powder at 300 °C was pulverized by a ball-milling process (Planetary Micro Mill, Pulverisette 7) for 6, 12, 15, and 18 h. The ball-milling process was conducted using balls of 1-mm diameter and a rotation speed of 500 rpm. To enhance the surface area, the steam activation method was performed. Ball-milled carbonized lignin powders were heated from room temperature to 1,000 °C at a ramping rate of 5 °C min^{-1} under N_2 flow (200 sccm) using a tube furnace. The activated carbon yield was approximately 22 wt%. The steam was injected into the furnace (10 ml h^{-1}) while the samples were held at 1000 °C for 1 h. The products were denoted as char lignin 6 h, char lignin 12 h, char lignin 15 h, and char lignin 18 h, depending on the ball-milling time. Following the steam activation, we named the products AC6, AC12, AC15, and AC18, respectively.

2. Characterizations

Thermogravimetric analysis (TGA) curves were obtained using Q50 (TA Instruments, USA) under N_2 flow of 100 ml min^{-1} at a ramping rate of 5 °C min^{-1} to 300 °C, followed by maintaining the temperature 5 h. The crystal structures of raw lignin and the carbonized lignin samples were investigated using X-ray diffraction (XRD, Smartlab 3, Rigaku, Japan) with Cu-Kα radiation at a scan rate of 5° min^{-1} from 5 to 80°. To analyze the morphologies, a scanning electron microscope (SEM, Nova Nano SEM 450, FEI, USA) was employed. The specific surface areas of the samples were cal-

culated using the Brunauer-Emmett-Teller technique with nitrogen adsorption on 3Flex (Micromeritics, USA) at 77 K after degassing the samples at 200 °C for 10 h. The pore size distribution was measured from the nitrogen isotherms using the Barrett-Joyner-Halenda (BJH) and Horvath-Kawazoe (HK) methods. The electrochemical performance of the AC samples was measured by the rotating disk electrode (RDE) method using an electrochemical workstation (AUT302M FRA2, Metrolhm Autolab, Netherlands). The active material (10 mg) was dispersed in a mixture of dimethylformamide (DMF, 1 ml), and Nafion (100 µl). An ink solution of 8 µl was dropped three times on a glassy carbon of area 0.196 cm^2, and dried at 60 °C. The loading mass of the dropped ink was approximately 0.25 mg. The drop-casted active material, Pt wire, and Ag/AgCl were used as the working, counter, and reference electrodes, respectively. Cyclic voltammetry (CV) curves were acquired using the RDE technique in 0.5 M H_2SO_4 at scan rates of 10, 20, 50, and 100 mV s^{-1} with a potential range of −0.2 to 0.8 V. The specific capacitance was calculated following Eq. (1):

$$C = \int IdV/2vmV \tag{1}$$

where I, V, v, and m represent the current, potential window, scan rate, and mass of active material, respectively.

Fig. S1 shows a schematic of the experimental setup for performing adsorption test. The adsorption of volatile organic compounds (VOCs) on the AC was studied in the tubular quartz reactor, which has an inner diameter of 1 cm. A mass of 300 mg of AC was put in the reactor and placed between ceramic fibers (Cerakwool, © KCC Co.). As shown in Fig. S1, nitrogen was bubbled through liquid toluene. The gas leaving the flask was saturated with toluene and then diluted by N_2 to control its concentration. The concentration of the diluted toluene was approximately 300 ppm, which was analyzed using on-line gas chromatography (GC, YL-6100, Young Lin Science) with a flame ionized detector (FID). The total flow rate of diluted toluene was 500 ml min^{-1}, and it was supplied to the reactor for 5 h. The increasing mass of AC after the test indicates the amount of adsorbed toluene. The adsorption capacity was calculated following Eq. (2).

$$\text{Adsorption capacity } (g_{toluene}/g_{AC})$$
$$= \frac{\text{AC after the test (g)} - \text{Fresh AC (g)}}{\text{Fresh AC (g)}} \tag{2}$$

RESULTS AND DISCUSSION

Prior to preparing the AC derived from lignin, we analyzed the thermal decomposition characteristics of lignin waste, which is a residue of biobutanol extraction from wood biomass, using TGA. This remains unclear, despite the many decomposition mechanisms of lignin that have been proposed over recent decades, owing to the complex and undefined structure of lignin [21,22]. Our lignin waste slowly decomposed over a broad temperature range from 110 to 600 °C, in three steps, because it contained oxygen of 23.7 at%, nitrogen of 0.7 at%, and sulfur of 0.6 at%, leading to scission of the lignin into small volatile molecules at different temperatures. The mass loss of the lignin started at 110 °C, corresponding to the evaporation of the contained water. The decomposition of polymeric
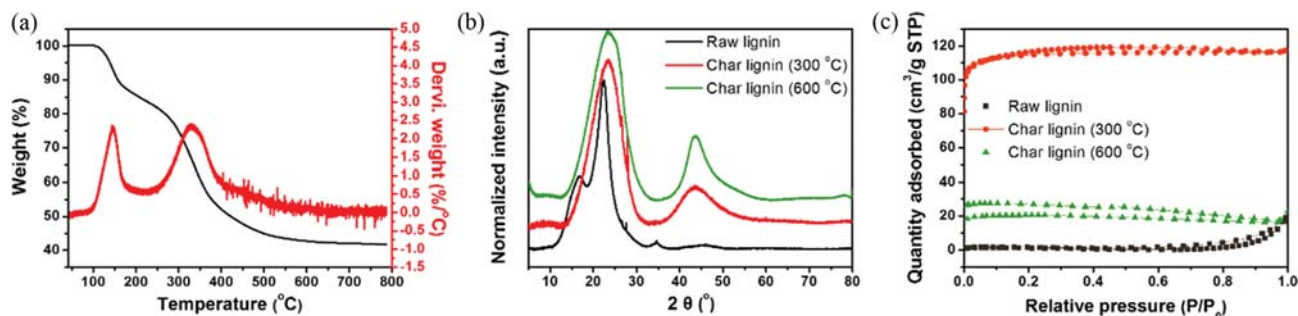
Fig. 1. (a) TGA curve of raw lignin in the temperature range of 40-800 °C under nitrogen atmosphere, (b) XRD patterns, and (c) physical adsorption isotherms (nitrogen) of raw lignin, and char lignins at 300, and 600 °C.
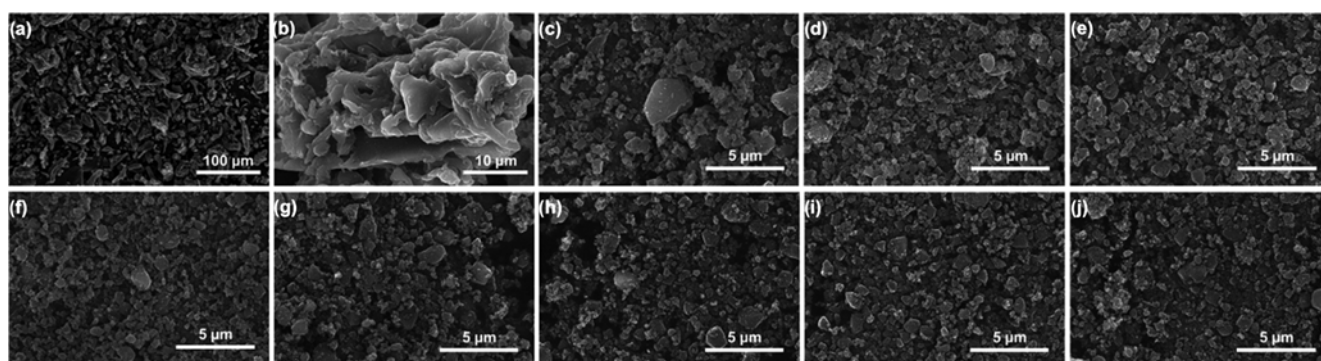

Fig. 2. SEM images of (a), (b) raw lignin, (c)-(f) char lignin carbonized at 300 °C, and (g)-(j) AC with different ball-milling times; (c), (g) 6 h, (d), (h) 12 h, (e), (i) 15 h, and (f), (j) 18 h.

lignin started at a relatively low temperature of approximately 220 °C. The main process of the thermal decomposition of polymeric lignin and removal of small volatile molecules occurred at approximately 330 °C, leading to the formation of aromatic hydrocarbons [23,24]. The char yield of the lignin was approximately 41.5 wt% after pyrolysis at 800 °C.

Considering the thermal decomposition characteristics of the lignin waste, the structural property of char lignin samples, which were prepared at the temperatures of 300 and 600 °C, were analyzed by XRD (Fig. 1(b)). In the X-ray diffractogram of raw lignin, the peaks at the 2θ angles of 16.7 and 22.4° are associated with the (110) and (200) planes of features of cellulose [25]. Interestingly, the peaks related to the cellulose shifted up to $2\theta=23.5$°, corresponding to the (002) plane of graphite, even though the char lignin samples were carbonized at a low temperature relative to the conventional carbonization of lignin. This might have originated from inter- or intramolecular crosslinking of polymeric chains, leading to the formation of aromatic hydrocarbons [26].

The specific surface area of the samples was analyzed using N_2 physisorption, as shown in Fig. 1(c) and Table S1. Raw lignin and char lignin carbonized at 300 and 600 °C showed values of 5.7, 455.5, and 81.9 m^2 g^{-1}, respectively. It might be expected that low-temperature carbonization affected the formation of the char lignin with large surface area, because of the remaining pore structure and self-activating using gasification of oxygen functional groups such as CO and CO_2. Some studies introduced a phenomenon that thermal annealing at relatively high temperature could lead to pore

collapse to decrease the surface area of carbon materials [27,28]. There was an observation of hysteresis with small deviations for the adsorption and desorption of N_2 gas, indicating the formation of pores.

Considering the char yields and surface area, we prepared AC using char lignin carbonized at 300 °C. The char lignin was ball-milled for various times from 6 to 18 h to increase the activation sites. Before ball-milling, the size of the char lignin was approximately 50 μm (Fig. 2). After ball-milling, the size significantly decreased below 2 μm. The char lignin samples ball-milled for longer than 12 h uniformly exhibited similar particle size. Ball-milling has no effect on the increased surface area of the samples, as summarized in Table S1. The ball-milled lignin char samples exhibited identical surface areas of approximately 480-490 m^2 g^{-1}, whereas the meso- and macro-pores increased with increasing ball-milling time (Fig. S2(a) and (b)).

The AC samples with different of ball-milling times were prepared under identical steam activation conditions. Fig. 3 shows the N_2 physisorption isotherms and pore size distributions for all the AC samples. Through the activation process, the surface area of all the samples significantly increased. Observing the surface morphology of the samples, AC6 shows a rigid surface, and the AC samples ball-milled for longer than 12 h have a highly porous morphology, as shown in Fig. S3. In particular, macroscale holes could be easily observed in AC18. Interestingly, AC12, which was prepared by carbonization at 300 °C, ball-milling for 12 h, and steam activation, exhibited the highest surface area (1075.2 m^2 g^{-1}) compared to
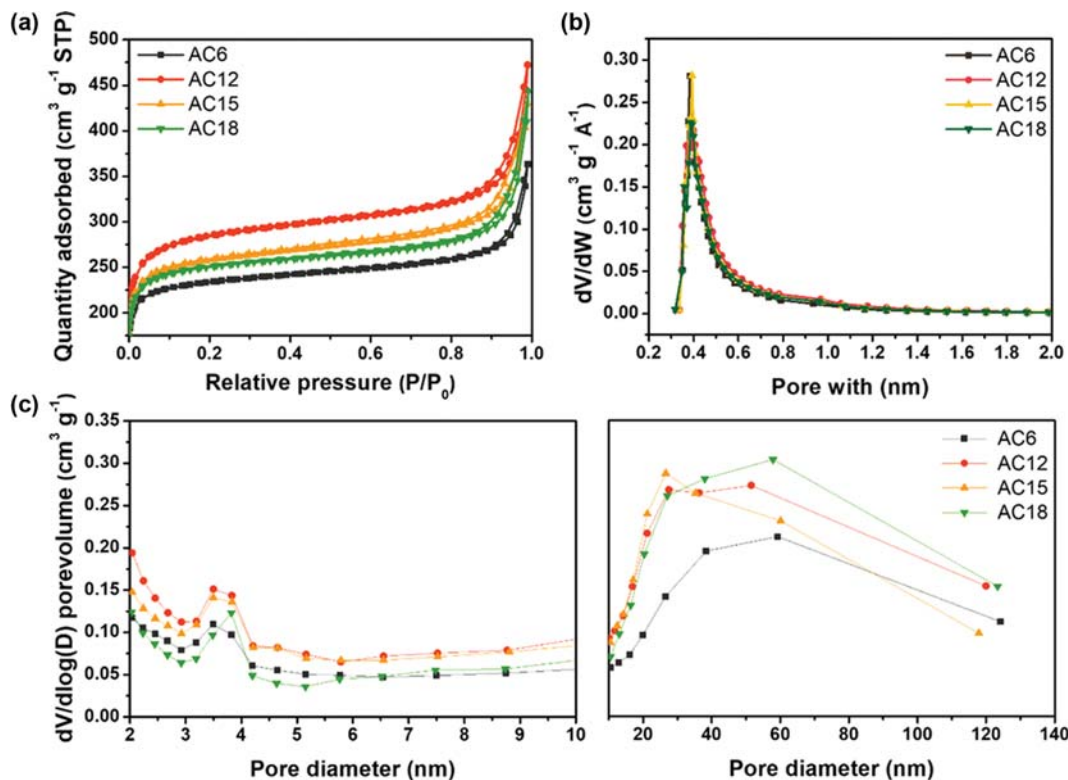
Fig. 3. Physical adsorption/desorption isotherms (N_2), (b) micro-pore size distribution, and (c) meso-pore size distribution calculated by H-K, and BJH methods of AC6, AC12, AC15, and AC18.

Table 1. Physical characteristics of ACs with respect to ball-milling time (6-18 h)

Sample	BET surface area ($m^2 g^{-1}$)	Micro pore volume ($cm^3 g^{-1}$)	Total pore volume ($cm^3 g^{-1}$)
AC6	907.78	0.366	0.563
AC12	1075.18	0.448	0.732
AC15	983.82	0.404	0.666
AC18	960.64	0.392	0.688

the other samples (Table 1). The meso- and micro-pore volumes of AC12 tend to be higher than those of the other samples. This might originate from the effect on the size of granules and pores. AC6 has the largest granules, leading to inefficient activation. Before activation, AC15 and 18 had higher pore volumes over all ranges of pore size, compared with AC12. After steam activation, their micropore volumes increased in relatively smaller increments. Azargohar et al. reported that the walls of the pores could be thinner or collapse when activation is conducted beyond a proper level, leading to a reduction in the surface area of the AC [29]. Therefore, we believed that there might be a complementary relationship between the surface area and morphological properties of lignin char.

The electrochemical properties of the all AC samples were investigated by CV in 0.5 H_2SO_4 electrolyte at a scan rate of 10, 20, 50 and 100 mV s^{-1} (Fig. 4). All the AC samples exhibited a rectangular CV curve, regardless of the scan rate, indicating an ideal capacitive behavior [3,4]. The specific adsorption characteristics of the AC samples were significantly improved compared with those before

activation (Fig. S2, and S4). AC12, with the largest surface area, and highest pore volume, showed a value of 115.1 F g^{-1} at a scan rate of 10 mV s^{-1}. Interestingly, only redox peaks for oxygen functional groups were weakly observed at approximately 0.3 V, even though the AC samples were activated using steam. To investigate the potential application of AC12 as adsorbents, we measured the adsorption quantity of the sample for toluene by the weighing method. AC12 exhibited a comparative adsorbability of 0.23 g$_{toluene}$ per g$_{activated\ carbon}$ [30]. Therefore, we believe that the as-synthesized AC could be a promising material for electrochemical electrodes and adsorbents of VOCs.

CONCLUSIONS

We synthesized AC derived from residual lignin waste from biobutanol extraction. Low-temperature carbonization can realize char lignin with high yields and surface area. Through a ball-milling process, a uniform morphology and enhanced activation sites of char lignin were achieved, with the result that time-consuming activation processes are longer required to compensate for the low reactivity of lignin chars. Cost-effective steam activation in a short period of time (4 h) finally leads to the formation of a highly porous structure and large surface area. As a result, the as-synthesized carbon materials exhibited a large surface area of 1,075.2 m^2 g^{-1}, high specific capacitance of 115.1 F g^{-1}, and excellent adsorbability of 0.23 g$_{toluene}$ per g$_{activated\ carbon}$. Therefore, we believe that the facile strategy presented here could lead to the realization of upcycling of lignin waste to highly useful AC.
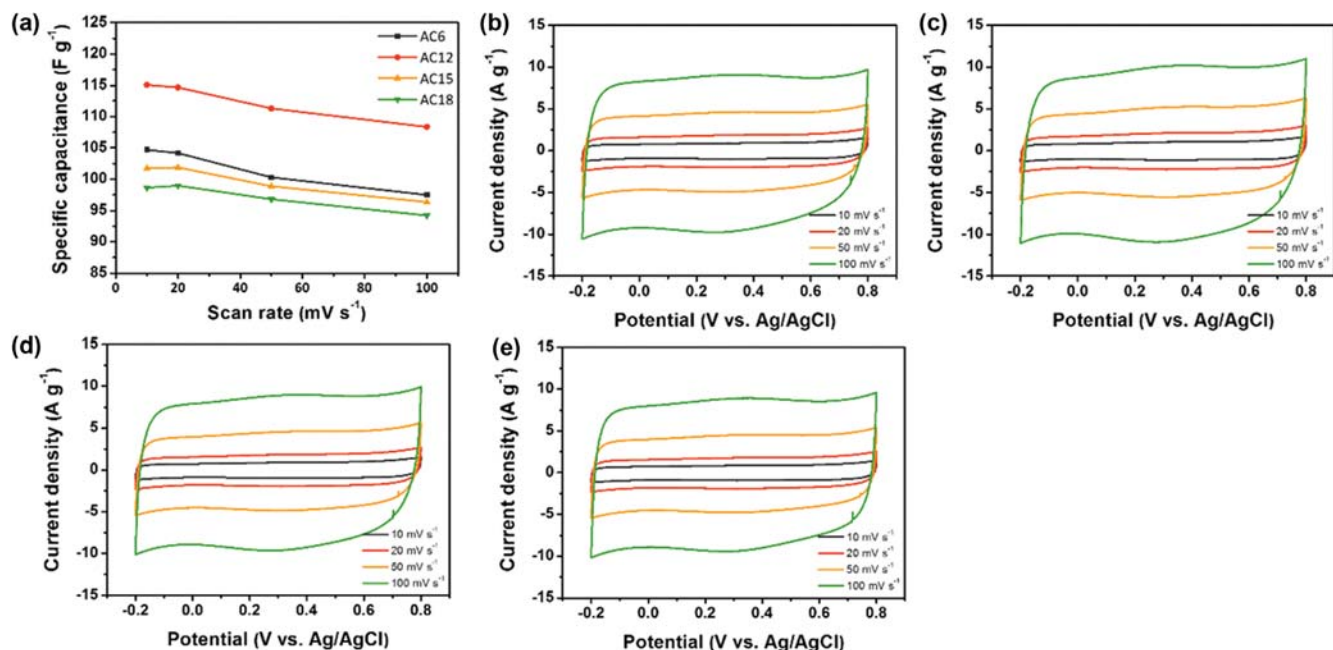
Fig. 4. (a) Specific capacitance of AC samples, and CV curves of (b) AC6, (c) AC12, (d) AC15, and (e) AC18 at scan rates of 10, 20, 50 and 100 mV s⁻¹.

SUPPORTING INFORMATION

Additional information as noted in the text. This information is available via the Internet at http://www.springer.com/chemistry/journal/11814.

REFERENCES

1. S. Chatterjee and T. Saito, *ChemSusChem.*, **8**, 3941 (2015).
2. A. Duval and M. Lawoko, *React. Funct. Polym.*, **85**, 78 (2014).
3. K. Barta, P. Anastas, E. Beach, T. Hansen, G. Warner and P. Foley, U.S. Patent, 10,059,650 (2018).
4. M. N. Belgacem and A. Gandini, Monomers, polymers and composites from renewable resources, Amsterdam, Elsevier (2008).
5. H.-I. Joh, H. K. Song, C.-H. Lee, J.-M. Yun, S. M. Jo, S. Lee, S.-I. Na, A.-T. Chien and S. Kumar, *Carbon*, **70**, 308 (2014).
6. H.-I. Joh, H. K. Song, K.-B. Yi and S. Lee, *Carbon*, **53**, 409 (2013).
7. S. Sircar, T. C. Golden and M. B. Rao, *Carbon*, **34**, 1 (1996).
8. P. J. M. Carrott and M. M. L. Ribeiro Carrott, *Bioresour. Technol.*, **98**, 2301 (2007).
9. Z. Gao, Y. Zhang, N. Song and X. Li, *Mater. Res. Lett.*, **5**, 69 (2017).
10. D. A and G. Hegde, *RSC Adv.*, **5**, 88339 (2015).
11. A. Kumar, H. Hegde, S. A. B. A. Manaf, Z. Ngaini and K. V. Sharma, *Chem. Commun.*, **50**, 12702 (2014).
12. E. Gonzalez-Serrano, T. Cordero, J. Rodriguez-Mirasol, L. Cotoruelo and J. J. Rodriguez, *Water Res.*, **38**, 3043 (2004).
13. R. J. Paterson, Lignin: properties and applications in biotechnology and bioenergy, Nova Science Publishers (2012).
14. S. Yorgun, N. Vural and H. Demiral, *Micropor. Mesopor. Mater.*, **122**, 189 (2009).
15. M. A. Lillo-Ródenas, D. Cazorla-Amorós and A. Linares-Solano, *Carbon*, **41**, 267 (2003).
16. T. Kou, B. Yao, T. Liu and Y. Li, *J. Mater. Chem. A.*, **5**, 17151 (2017).
17. X. Ma, H. Yang, L. Yu, Y. Chen and Y. Li, *Materials*, **7**, 4431 (2014).
18. J. Rodriguez-Mirasol, T. Cordero and J. J. Rodriguez, *Energy Fuels*, **7**, 133 (1993).
19. X. Xie, B. Goodell, D. Zhang, D. C. Nagle, Y. Qian, M. L. Peterson and J. Jellison, *Bioresour. Technol.*, **100**, 1797 (2009).
20. M. Kijima, T. Hirukawa, F. Hanawa and T. Hata, *Bioresour. Technol.*, **102**, 6279 (2011).
21. M. Brebu, G. Cazacu and O. Chirila, *Cell. Chem. Technol.*, **45**, 43 (2011).
22. M. Brebu and C. Vasile, *Cell. Chem. Technol.*, **44**, 353 (2010).
23. R. Alén, E. Kuoppala and P. Oesch, *J. Anal. Appl. Pyrolysis*, **36**, 137 (1996).
24. J. Rodrigues, J. Graça and H. Pereira, *J. Anal. Appl. Pyrolysis*, **58-59**, 481 (2001).
25. D. Yang, L.-X. Zhong, T.-Q. Yuan, X.-W. Peng and R.-C. Sun, *Ind. Crop. Prod.*, **43**, 141 (2013).
26. K. Oh, S. Lee, S. Park, B.-C. Ku, S. H. Lee, Y. H. Bang and H.-I. Joh, *Sci. Adv. Mater.*, **9**, 1566 (2017).
27. E. Arenas and F. Chejne, *Carbon*, **42**, 2451 (2004).
28. A. Zolin, A. D. Jensen, P. A. Jensen and K. Dam-Johansen, *Fuel*, **81**, 1065 (2002).
29. R. Azargohar and A. K. Dalai, *Micropor. Mesopor. Mater.*, **85**, 219 (2005).
30. M. J. Lashaki, M. Fayaz, H. Wang, Z. Hashisho, J. H. Philips, J. E. Anderson and M. Nichols, *Environ. Sci. Technol.*, **46**, 4083 (2012).